symmetry

IMPACT FACTOR 2.940

CITESCORE 4.3

Article

Quantum Speed-Up Induced by the Quantum Phase Transition in a Nonlinear Dicke Model with Two Impurity Qubits

Wangjun Lu, Cuilu Zhai, Yan Liu, Yaju Song, Jibing Yuan, Songsong Li and Shiqing Tang

Special Issue
New Frontiers in Quantum Information

Edited by
Prof. Dr. Wuming Liu and Dr. Xingdong Zhao

MDPI

https://doi.org/10.3390/sym14122653

symmetry

Article

Quantum Speed-Up Induced by the Quantum Phase Transition in a Nonlinear Dicke Model with Two Impurity Qubits

Wangjun Lu [1,2,3], Cuilu Zhai [1], Yan Liu [2], Yaju Song [2], Jibing Yuan [2], Songsong Li [4] and Shiqing Tang [2,*]

1 Department of Maths and Physics, Hunan Institute of Engineering, Xiangtan 411104, China
2 College of Physics and Electronic Engineering, Hengyang Normal University, Hengyang 421002, China
3 Zhejiang Institute of Modern Physics, Department of Physics, Zhejiang University, Hangzhou 310027, China
4 College of Physics and Electronic Information, Nanchang Normal University, Nanchang 330032, China
* Correspondence: sqtang@hynu.edu.cn

Abstract: In this paper, we investigate the effect of the Dicke quantum phase transition on the speed of evolution of the system dynamics. At the phase transition point, the symmetry associated with the system parity operator begins to break down. By comparing the magnitudes of the two types of quantum speed limit times, we find that the quantum speed limit time of the system is described by one of the quantum speed limit times, whether in the normal or superradiant phase. We find that, in the normal phase, the strength of the coupling between the optical field and the atoms has little effect on the dynamical evolution speed of the system. However, in the superradiant phase, a stronger atom–photon coupling strength can accelerate the system dynamics' evolution. Finally, we investigate the effect of the entanglement of the initial state of the system on the speed of evolution of the system dynamics. We find that in the normal phase, the entanglement of the initial state of the system has almost no effect on the system dynamics' evolution speed. However, in the superradiant phase, larger entanglement of the system can accelerate the evolution of the system dynamics. Furthermore, we verify the above conclusions by the actual evolution of the system.

Keywords: quantum speed limit time; Dicke quantum phase transition; normal phase; superradiant phase; entanglement

Citation: Lu, W.; Zhai, C.; Liu, Y.; Song, Y.; Yuan, J.; Li, S.; Tang, S. Quantum Speed-Up Induced by the Quantum Phase Transition in a Nonlinear Dicke Model with Two Impurity Qubits. *Symmetry* **2022**, *14*, 2653. https://doi.org/10.3390/sym14122653

Academic Editors: Wuming Liu and Xingdong Zhao

Received: 27 October 2022
Accepted: 8 December 2022
Published: 15 December 2022

1. Introduction

The quantum speed limit (QSL) characterizes the lower bound on the minimum time a quantum system can take to evolve from an initial quantum state to a distinguishable state [1–9]. The quantum speed limit has important application value in various research fields of quantum physics, such as quantum communication [10–15], quantum computing [16–19], quantum metrology [20–23], non-equilibrium thermodynamics [24–26], and quantum optimal control theory [4,27–32]. Currently, there are two main understandings of quantum acceleration. The first understanding is that the shorter the quantum speed limit time is, the faster the quantum system evolves, given the fidelity between the initial and final states. The second one is based on comparing the quantum speed limit time and the actual evolution time. If the actual evolution time is equal to the quantum speed limit time, it means that the system has evolved along the fastest path and the system has no potential to accelerate. However, if the actual evolution time is greater than the quantum speed limit time, the system has the potential to accelerate [33–42].

For a closed quantum system, the dynamical evolution is determined by a time-independent Hamiltonian $\hat{H}$ when the system evolves from an initial state to an orthogonal state of the initial state. Mandelstam and Tamm (MT) obtained a quantum speed limit determined by the system's Hamiltonian variance based on the Cauchy–Schwarz inequality [43]. This limit shows that the speed limit time τ_{MT} required for the system to evolve from the initial state to the orthogonal state of the initial state satisfies the equation $\tau_{MT} = \pi\hbar/(2\Delta\hat{H})$, where $\Delta\hat{H}$ denotes the variance of the Hamiltonian $\hat{H}$ over the initial state. In 1998, Margolus and Levitin (ML) obtained another quantum speed limit time using the von Neumann trace inequality [18,44]. They showed that the limit time τ_{ML} required for a closed quantum system to evolve from its initial state to its orthogonal state satisfies the equation $\tau_{MT} = \pi\hbar/[2(\langle\hat{H}\rangle - E_0)]$. $\langle\hat{H}\rangle$ and E_0 are the mean value of Hamiltonian $\hat{H}$ over the initial state and the ground state energy of Hamiltonian $\hat{H}$, respectively. Both MT-type and ML-type quantum speed limits indicate that the time required for a quantum system to evolve from its initial state to its orthogonal state depends only on the initial state of the quantum system and the system's Hamiltonian. The time required for a closed quantum system to evolve from its initial state to its orthogonal state must satisfy both MT-type and ML-type quantum speed limit times. Thus, the quantum speed limit time of the system is taken as the largest of the two. That is, the quantum speed limit time of the system is $\tau_{QSL} = \max\{\pi\hbar/(2\Delta\hat{H}), \pi\hbar/[2(\langle\hat{H}\rangle - E_0)]\}$ [18]. It is worth noting that the MT-type and ML-type quantum speed limit times are only applicable to closed quantum systems whose initial state is a pure state. In recent years, the quantum speed limit time has been extended to systems with mixed initial states and open systems [3,33,38,45–58].

In quantum computing, quantum communication, and quantum simulation, the control of the dynamical evolution speed of the system is critical. Moreover, quantum phase transitions can strongly influence the dynamical behavior of the system [59–82]. Meanwhile, continuous-variable entanglement, a key resource in continuous-variable quantum information processing, has been widely used in various quantum communications and quantum computing [83–90]. The effect of the Dicke quantum phase transition as an environment on the quantum speed limit time of a two-level atom has been studied [91]. Here, we mainly study the effects of quantum phase transition and initial state entanglement on the quantum speed limit time of the system. We find that, in the normal phase, the phase transition parameters and the initial state entanglement of the system have almost no effect on the quantum speed limit time. However, in the superradiant phase, both the phase transition parameters and the initial state entanglement can accelerate the system's dynamical evolution. Finally, we confirm these conclusions through the actual dynamical evolution of the system.

2. Quantum Phase Transition in a Nonlinear Dicke Model with Two Impurity Qubits

In this section, we focus on the quantum phase transition of the nonlinear Dicke model containing two impurity qubits. Here, the two impurity qubits interact only with the single-mode optical field in the nonlinear Dicke model. The interaction of the two impurity qubits with the single-mode optical field is described by the following Tavis–Cummings model:

$$\hat{H}_{TC} = \omega_a\hat{a}^\dagger\hat{a} + \frac{\omega_q}{2}\sum_{i=1,2}\hat{\sigma}_z^i + g\sum_{i=1,2}(\hat{a}^\dagger\hat{\sigma}_-^i + \hat{\sigma}_+^i\hat{a}), \tag{1}$$

where $\hat{a}$ ($\hat{a}^\dagger$) is the annihilation (creation) operator of the single-mode cavity field with resonance frequency ω_a and ω_q is the transition frequency between the two levels of the impurity qubit. $\hat{\sigma}^i_{x,y,z}$ are the usual Pauli operators of the impurity qubit, and $\hat{\sigma}^i_\pm = \frac{1}{2}(\hat{\sigma}^i_x \pm i\hat{\sigma}^i_y)$. g is the dipole interaction strength between the cavity field and the impurity qubit. We define a frequency detuning $\Delta_q = \omega_q - \omega_a$. Under the large detuning condition, i.e., $\Delta_q \gg g$, the Hamiltonian above can be transformed by the Fröhlich–Nakajima transformation into the following form [92,93]:

$$\hat{H}^{eff}_{TC} = \omega_a\hat{a}^\dagger\hat{a} + \frac{\omega_q}{2}\sum_{i=1,2}\hat{\sigma}_z^i + \sum_{i=1,2}\kappa_i\hat{a}^\dagger\hat{a}\hat{\sigma}_z^i, \tag{2}$$

where $\kappa_i = g^2/\Delta_q$. The Hamiltonian of the nonlinear Dicke model is

$$\hat{H}_D = \omega_a\hat{a}^\dagger\hat{a} + \omega_0\hat{J}_z + \frac{\lambda}{\sqrt{N}}(\hat{a}^\dagger + \hat{a})(\hat{J}_+ + \hat{J}_-) + \frac{\chi}{N}\hat{J}_z^2, \tag{3}$$

where ω_0 is the transition frequency of these N identical two-level atoms. $\hat{J}_j$ $(j = x, y, z)$ is the collective angular momentum operator for the spin ensemble consisting of N identical two-level atoms; these operators $\hat{J}_x, \hat{J}_y, \hat{J}_z$ satisfy the commutation relation of the $SU(2)$ algebra and $\hat{J}_\pm = \hat{J}_x \pm i\hat{J}_y$. χ denotes the interaction between N identical two-level atoms.

When both the interaction of the two impurity qubits with the light field and the interaction between the atoms vanish, the above equation is reduced to the standard Dicke model. Then, the Hamiltonian of the nonlinear Dicke model with two impurity qubits is as follows:

$$\hat{H} = \hat{H}_D + \frac{\omega_q}{2}\sum_{i=1,2}\hat{\sigma}_z^i + \sum_{i=1,2}\kappa_i\hat{a}^\dagger\hat{a}\hat{\sigma}_z^i. \tag{4}$$

With the Holstein–Primakoff transformation [94], we can represent the angular momentum operators by the following single-mode boson operators:

$$\hat{J}_+ = \hat{c}^\dagger\sqrt{N - \hat{c}^\dagger\hat{c}}, \quad \hat{J}_- = \sqrt{N - \hat{c}^\dagger\hat{c}}\hat{c}, \quad \hat{J}_z = \hat{c}^\dagger\hat{c} - \frac{N}{2}. \tag{5}$$

Substituting Equation (5) into Equation (4) and dropping the constant terms and conserved term yield

$$\begin{aligned}\hat{H} &= \left(\omega_a + \sum_{i=1,2}\kappa_i\hat{\sigma}_z^i\right)\hat{a}^\dagger\hat{a} + (\omega_0 - \chi)\hat{c}^\dagger\hat{c} + \lambda(\hat{a}^\dagger + \hat{a})\left(\hat{c}^\dagger\sqrt{1 - \frac{\hat{c}^\dagger\hat{c}}{N}} + \sqrt{1 - \frac{\hat{c}^\dagger\hat{c}}{N}}\hat{c}\right) \\ &\quad + \frac{\chi}{N}(\hat{c}^\dagger\hat{c})^2. \end{aligned}\tag{6}$$

To describe the collective behavior of condensed atoms and photons, we introduce new boson operators $\hat{a}_1 = \hat{a} + \sqrt{N}\alpha$ and $\hat{c}_1 = \hat{c} - \sqrt{N}\beta$, where both α and β are real numbers. Substituting $\hat{a}_1$ and $\hat{c}_1$ into the above equation and neglecting the term of N in the denominator yields the following expression:

$$\hat{H} = NE_0 + \sqrt{N}\hat{H}_1 + \hat{H}_2, \tag{7}$$

where E_0, $\hat{H}_1$, and $\hat{H}_2$ are defined by

$$E_0 = \omega_a'\alpha^2 + (\omega_0 - \chi)\beta^2 + \chi\beta^4 - 4\lambda\sqrt{1 - \beta^2}\alpha\beta, \tag{8}$$

$$\begin{aligned}\hat{H}_1 &= \left[2\lambda\alpha\frac{1 - 2\beta^2}{\sqrt{1 - \beta^2}} - (\omega_0 - \chi)\beta - 2\chi\beta^3\right]\left(c_1^\dagger + c_1\right) \\ &\quad + \left[\omega_a'\alpha - 2\lambda\sqrt{1 - \beta^2}\beta\right]\left(a_1^\dagger + a_1\right),\end{aligned}\tag{9}$$

$$\begin{aligned}\hat{H}_2 &= \omega_a' a_1^\dagger a_1 + \left[(\omega_0 - \chi) + 2\chi\beta^2 + \frac{2\lambda\alpha\beta}{\sqrt{1 - \beta^2}}\right]c_1^\dagger c_1 \\ &\quad + \left[\chi\beta^2 + \frac{\lambda\alpha\beta(2 + \beta^2)}{2(1 - \beta^2)\sqrt{1 - \beta^2}}\right]\left(c_1^\dagger + c_1\right)^2 - \frac{\lambda\alpha\beta}{\sqrt{1 - \beta^2}} \\ &\quad + \frac{\lambda(1 - 2\beta^2)(a_1^\dagger + a_1)(c_1^\dagger + c_1)}{\sqrt{1 - \beta^2}}.\end{aligned}\tag{10}$$

Here, $\omega_a' = \omega_a + \sum_{i=1,2}\kappa_i\langle\hat{\sigma}_z^i\rangle$. Since $\hat{\sigma}_z^i$ commutes with the total Hamiltonian $\hat{H}$, we replace $\hat{\sigma}_z^i$ with its mean $\langle\hat{\sigma}_z^i\rangle$.

The collective excitation parameters α, β can be determined from the equilibrium conditions $\partial E_0/\partial\alpha = 0$, $\partial E_0/\partial\beta = 0$, which leads to the following two equations:

$$\omega_a'\alpha - 2\lambda\sqrt{1 - \beta^2}\beta = 0, \tag{11}$$

$$(\omega_0 - \chi)\beta + 2\chi\beta^3 - \frac{2\lambda\alpha(1-2\beta^2)}{\sqrt{1-\beta^2}} = 0. \quad (12)$$

In this way, we are able to obtain an equation that characterizes the quantum phase transition:

$$\beta\left[\left(2\chi\omega'_a + 8\lambda^2\right)\beta^2 + \omega'_a(\omega_0 - \chi) - 4\lambda^2\right] = 0. \quad (13)$$

Obviously, if $\omega'_a(\omega_0 - \chi) - 4\lambda^2 > 0$, then $\beta = \alpha = 0$, i.e., there is no macroscopic excitation of both the light field and the atoms. At this point, the system is in the normal phase. However, when $\omega'_a(\omega_0 - \chi) - 4\lambda^2 < 0$, then we can obtain the following expression:

$$\alpha^2 = \frac{\lambda^2}{\omega'^2_a} - \frac{\lambda^2\omega_0^2}{(4\lambda^2 + \chi\omega'_a)^2}, \quad (14)$$

$$\beta^2 = \frac{1}{2} - \frac{\omega'_a\omega_0}{8\lambda^2 + 2\chi\omega'_a}. \quad (15)$$

Equations (14) and (15) imply the existence of macroscopic excitations in the light field and the atoms, respectively. In this case, the system is in the superradiant phase. At the transition point from the normal phase to the superradiant phase, the symmetry of the ground state of the system defined by the parity operator $\hat{\Pi} = \exp[i\pi(\hat{a}^\dagger\hat{a} + \hat{J}_z + N/2)]$ is broken. This spontaneous symmetry breaking was studied in [60].

In the thermodynamic limit $N \to \infty$, we can obtain the scaled population inversion of N identical two-level atoms as

$$\frac{\langle J_z\rangle}{N} = \beta^2 - \frac{1}{2} = -\frac{\omega'_a\omega_0}{8\lambda^2 + 2\chi\omega'_a}. \quad (16)$$

In Figure 1, we plot the variation of the atomic population with the strength of interatomic interactions and atom–photon interactions. When $\langle\hat{J}_z\rangle/N = -0.5$, the atoms have no macroscopic population in the excited state, and the system is in the normal phase. When $\langle\hat{J}_z\rangle/N > -0.5$, there is macroscopic excitation of the atoms, and the system is in the superradiant phase. The red line indicates the dividing line between the normal phase and the superradiant phase. The relevant parameters in Figure 1 were selected from [95].

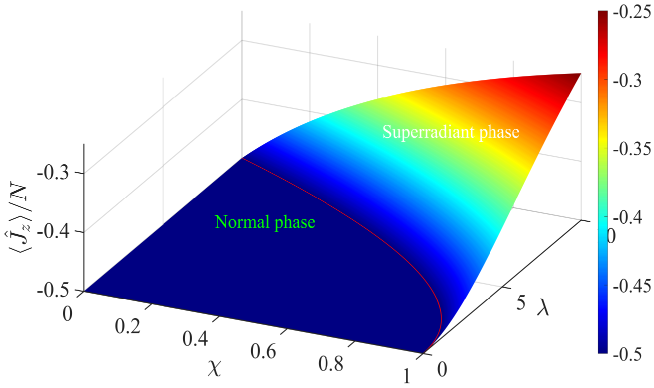

Figure 1. Phase diagrams described by the scaled population inversion of $\langle\hat{J}_z\rangle/N$ with respect to the atom–photon coupling strength λ and interatomic interaction χ. The other parameters are taken as $\omega_a = 20$MHz, $\omega_0 = 0.05$MHz, $N = 10^5$, and both qubits are in the ground state $|g\rangle \otimes |g\rangle$. The relevant parameters in the figure are given in units of ω_0.

3. The Effect of Quantum Phase Transition on Quantum Speed Limit Time

In this section, we focus on the effect of the Dicke quantum phase transition on the speed of evolution of the system dynamics. For a closed system, its initial and orthogonal states are $|\Psi(0)\rangle$ and $|\Psi(\tau)\rangle$, respectively. Then, the quantum speed limit time for this closed system to evolve from the initial state to the orthogonal state is given by the following equation [18]:

$$\tau_{QST} = \max\{\tau_{MT}, \tau_{ML}\}. \tag{17}$$

Furthermore, τ_{QST} has been shown to be tightly bounded [18].

In the following, for an initial state $|\Psi(0)\rangle$ of the system, we discuss the quantum speed limit time of the system in the normal phase and superradiant phase regions, respectively. For a given initial state,

$$|\Psi(0)\rangle = W[\cos\theta|\gamma,\eta\rangle + \sin\theta\exp(i\varphi)|-\gamma,-\eta\rangle], \tag{18}$$

where $\theta \in [0,\pi/2], \varphi \in [0,2\pi]$ and $|\gamma\rangle$ and $|-\gamma\rangle$ ($|\eta\rangle$ and $|-\eta\rangle$) are the eigenstates of the operator annihilation operators $\hat{a}$ ($\hat{c}$) when the eigenvalues are γ and $-\gamma$ (η and $-\eta$), respectively. Obviously, $|\Psi(0)\rangle$ is a superposition state of coherent states. The normalization coefficient is given by the following equation:

$$W^2 = [1 + K\cos\varphi\sin 2\theta]^{-1}, \tag{19}$$

where $K = \exp\left[-2\left(|\gamma|^2 + |\eta|^2\right)\right]$.

In the normal phase at the thermodynamic limit $N \to \infty$, we can take $\frac{\hat{c}^\dagger\hat{c}}{N} \approx 0$, $\frac{(\hat{c}^\dagger\hat{c})^2}{N} \approx 0$. Hamiltonian Equation (6) then becomes

$$\hat{H_{np}} = \omega_a'\hat{a}^\dagger\hat{a} + (\omega_0 - \chi)\hat{c}^\dagger\hat{c} + \lambda\left(\hat{a}^\dagger + \hat{a}\right)\left(\hat{c}^\dagger + \hat{c}\right). \tag{20}$$

Since neither the atoms nor the light field is collectively excited in the normal phase, the ground state energy of the system in the normal phase in the thermodynamic limit is $E_0 = 0$. For our studied nonlinear Dicke quantum system with two impurity qubits in the normal phase, the limit time for the system to evolve from the initial state $|\Psi(0)\rangle$ to the orthogonal state of the initial state is

$$\tau_{np} = \max\left\{\frac{\pi}{2\sqrt{\langle\hat{H}_{np}^2\rangle - \langle\hat{H}_{np}\rangle^2}}, \frac{\pi}{2\langle\hat{H}_{np}\rangle}\right\}, \tag{21}$$

where the average value of the Hamiltonian $\hat{H}_{np}$ over the initial state $|\Psi(0)\rangle$ is

$$\langle\hat{H}_{np}\rangle \quad = \quad W^2[(R + 4\lambda\mathrm{Re}(\gamma)\mathrm{Re}(\eta)) - D(R + 4\lambda\mathrm{Im}(\gamma)\times\mathrm{Im}(\eta))], \tag{22}$$

and $R = \omega_a'|\gamma|^2 + (\omega_0 - \chi)|\eta|^2$, $D = K\sin 2\theta\cos\varphi$. The average value of $\hat{H}_n^2$ over the initial state $|\Psi(0)\rangle$ is

$$\begin{aligned} &\langle\hat{H}_{np}^2\rangle \\ = \quad & W^2\Big\{\omega_a'^2F(\gamma) + (\omega_0-\chi)^2F(\eta) + \lambda^2[\Pi_+ + D\Pi_-] + 2\omega_a'(\omega_0-\chi)|\gamma|^2|\eta|^2(1+D) \\ & +4(\omega_0-\chi)\lambda\left[\left(2|\eta|^2+1\right)\mathrm{Re}(\gamma)\mathrm{Re}(\eta) + D\mathrm{Im}(\gamma)\mathrm{Im}(\eta)\left(2|\eta|^2-1\right)\right] \\ & +4\omega_a'\lambda\left[\left(2|\gamma|^2+1\right)\mathrm{Re}(\gamma)\mathrm{Re}(\eta) + D\mathrm{Im}(\gamma)\mathrm{Im}(\eta)\left(2|\gamma|^2-1\right)\right]\Big\}, \end{aligned} \tag{23}$$

where

$$F(j) \quad = \quad |j|^2\left[\left(|j|^2+1\right)\left(1-|j|^2\right)\right], j = \gamma, \eta, \tag{24}$$

$$\Pi_{\pm} = \left(2\mathrm{Re}\left(\gamma^2\right) \pm 2|\gamma|^2 + 1\right)\left(2\mathrm{Re}\left(\eta^2\right) \pm 2|\eta|^2 + 1\right). \tag{25}$$

In the superradiant phase, we translate the two operators, $\hat{a}$ and $\hat{c}$, respectively, where $\hat{a} = \hat{a}_1 - \sqrt{N}\alpha, \hat{c} = \hat{c}_1 + \sqrt{N}\beta$. The values of α and β are determined by Equations (14) and (15), respectively. Substitute the operators after the translation into Equation (6). Because, in the thermodynamic limit $N \to \infty$, the denominator terms containing N have a value of zero, after neglecting the terms of N in the denominator and the constant terms, we obtain

$$\hat{H}_{sp} = \omega_a' \hat{a}_1^\dagger \hat{a}_1 + \tilde{\omega}_0 \hat{c}_1^\dagger \hat{c}_1 + \lambda_1 \left(\hat{a}_1^\dagger + \hat{a}_1\right)\left(\hat{c}_1^\dagger + \hat{c}_1\right) + \lambda_2 \left(\hat{c}_1^\dagger + \hat{c}_1\right)^2, \tag{26}$$

where the parameters $\tilde{\omega}_0$, λ_1, and λ_2 are given by

$$\tilde{\omega}_0 = \frac{2\lambda^2\omega_0}{4\lambda^2 + \chi\omega_a'} + \frac{2\lambda^2}{\omega_a'}, \tag{27}$$

$$\lambda_1 = \frac{\lambda\omega_a'\omega_0}{\sqrt{(4\lambda^2 + \chi\omega_a')(4\lambda^2 + \chi\omega_a' + \omega_a'\omega_0)}}, \tag{28}$$

$$\lambda_2 = \frac{\lambda^2}{2\omega_a'}\frac{(1-\mu)(3+\mu)}{1+\mu} + \frac{\chi}{2}(1-\mu). \tag{29}$$

Since $\hat{a_1}$ and $\hat{c_1}$ are the operators after displacing the bosonic operators $\hat{a}$ and $\hat{c}$, respectively, then, we obtain the eigenvalues of $\hat{a_1}$ ($\hat{c_1}$) for the states $|\gamma\rangle$ and $|-\gamma\rangle$ ($|\eta\rangle$ and $|-\eta\rangle$), respectively.

$$\hat{a_1}|\gamma\rangle = (\hat{a} + \sqrt{N}\alpha)|\gamma\rangle = A_1|\gamma\rangle, \tag{30}$$

$$\hat{a_1}|-\gamma\rangle = (\hat{a} + \sqrt{N}\alpha)|-\gamma\rangle = A_2|-\gamma\rangle, \tag{31}$$

$$\hat{c_1}|\eta\rangle = (\hat{c} - \sqrt{N}\beta)|\eta\rangle = B_1|\eta\rangle, \tag{32}$$

$$\hat{c_1}|-\eta\rangle = (\hat{c} - \sqrt{N}\beta)|-\eta\rangle = B_2|-\eta\rangle, \tag{33}$$

where $A_1 = \gamma + \sqrt{N}\alpha$, $A_2 = -\gamma + \sqrt{N}\alpha$, $B_1 = \eta - \sqrt{N}\beta$, and $B_2 = -\eta - \sqrt{N}\beta$.

In the superradiant phase, the ground state energy of the system is given by Equation (8). Then, for the following quantum speed limit time:

$$\tau_{QSL} = \max\left\{\frac{\pi}{2\sqrt{\langle\hat{H}_{sp}^2\rangle - \langle\hat{H}_{sp}\rangle^2}}, \frac{\pi}{2(\langle\hat{H}_{sp}\rangle - E_0)}\right\}. \tag{34}$$

We need to calculate the average values of $\hat{H}_{sp}$ and $\hat{H}_{sp}^2$ on the initial state $|\Psi(0)\rangle$. We easily obtain the average value of $\hat{H}_{sp}$ over the initial state $|\Psi(0)\rangle$ as

$$\begin{aligned}\langle\hat{H}_{sp}\rangle = {} & W^2\Bigg\{\sum_{j=1,2}(-1)^{j-1}\sin(\theta + j\frac{\pi}{2})\Big[\omega_a|A_j|^2 + \tilde{\omega}_0|B_j|^2 + 4\lambda_1\mathrm{Re}(A_j)\mathrm{Re}(B_j) \\ & + \lambda_2\left(2\mathrm{Re}\left(B_j^2\right) + 2|B_j|^2 + 1\right)\Big] + K\sin 2\theta\mathrm{Re}\{\exp(i\varphi)[\omega_a A_1^* A_2 + \tilde{\omega}_0 B_1^* B_2 \\ & + \lambda_1(A_1^* + A_2)(B_1^* + B_2) + \lambda_2\left(B_1^{*2} + B_2^2 + 2B_1^* B_2 + 1\right)]\}\Bigg\}. \end{aligned} \tag{35}$$

Since the average value of $\hat{H}_{sp}^2$ over the initial state $|\Psi(0)\rangle$ is too cumbersome, we put it in Appendix A.

In order to determine the quantum speed limit times of the system in the normal and superradiant phases, we need to compare the magnitude of the MT-type and ML-type quantum speed limit times. In Figure 2a, when $\omega_a = 400\omega_0$, $\chi = 0.64\omega_0$, we plot the variation of these two quantum speed limit times with the phase transition parameter λ. The figure shows that the MT-type quantum speed limit time is always larger than the ML-type quantum speed limit time, whether in the normal phase region or the superradiant phase region. Furthermore, to investigate whether the MT-type quantum speed limit time is always larger than the ML-type quantum speed limit time at different interatomic interaction strengths, we plot the variation of the two quantum speed limit times with the phase transition parameter λ and the interatomic interaction strength χ in Figure 2b. We find that the MT-type quantum speed limit time is always larger than the ML-type quantum speed limit time in any parameter interval, so we can obtain the quantum speed limit time of the system as follows:

$$\tau_{QSL} = \begin{cases} \dfrac{\pi}{2\sqrt{\langle \hat{H}_{np}^2 \rangle - \langle \hat{H}_{np} \rangle^2}}, & \textbf{Normal phase}, \\ \dfrac{\pi}{2\sqrt{\langle \hat{H}_{sp}^2 \rangle - \langle \hat{H}_{sp} \rangle^2}}, & \textbf{Superradiant phase}. \end{cases} \tag{36}$$

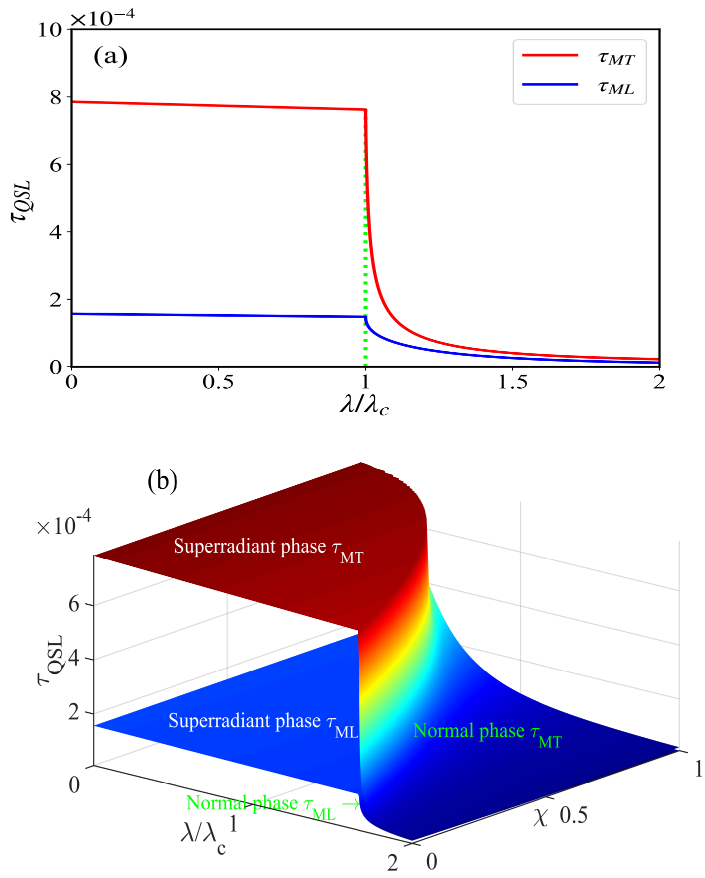

Figure 2. (**a**) Variation of MT-type and ML-type quantum speed limit times with the phase transition parameter λ, where $\omega_a = 400\omega_0$, $\chi = 0.64\omega_0$, and the critical coupling strength $\lambda_c = 6\omega_0$. (**b**) The MT-type and ML-type quantum speed limit times vary with the phase transition parameter λ and the strength χ of the interatomic interactions. The initial state parameters of the system are $\gamma = \eta = 5$, $\varphi = 0$, and $\theta = \pi/4$. The other parameters are the same as in Figure 2.

From Figure 2a,b, we can see a sudden change in the quantum speed limit time of the system from the normal phase to the superradiant phase. Moreover, the stronger the coupling between the optical field and the atoms, the smaller the quantum speed limit time is, which means that the stronger interaction between the subsystems can accelerate the evolution of the system dynamics. At the same time, in the normal phase, the quantum speed limit time of the system decreases slowly with the increase of the phase transition parameter λ. However, once the coupling strength λ exceeds the critical coupling strength λ_c, in the superradiant phase, the quantum speed limit time of the system suddenly decreases sharply. Moreover, when the coupling strength λ far exceeds the critical coupling strength λ_c, the quantum speed limit time of the system again decreases slowly with the increase of the phase transition parameter λ.

In order to verify our conclusions from the actual dynamical evolution of the system, in Figure 3, we plot the fidelity of the initial state of the system with time for different phase transition parameters. We find that, in the normal phase region, the time taken for the system to evolve from the initial state to the orthogonal state of the initial state hardly decreases with the enhancement of the coupling strength. However, in the superradiant phase, the time for the system to reach the initial state's orthogonal state decreases with the coupling strength. In other words, in the normal phase, the stronger phase transition parameters hardly accelerate the system dynamics' evolution. In contrast, the stronger phase transition parameters accelerate the system dynamics' evolution in the superradiant phase. The numerical simulation of the actual dynamical evolution of the system in Figure 3 was performed with the Qutip software [96].

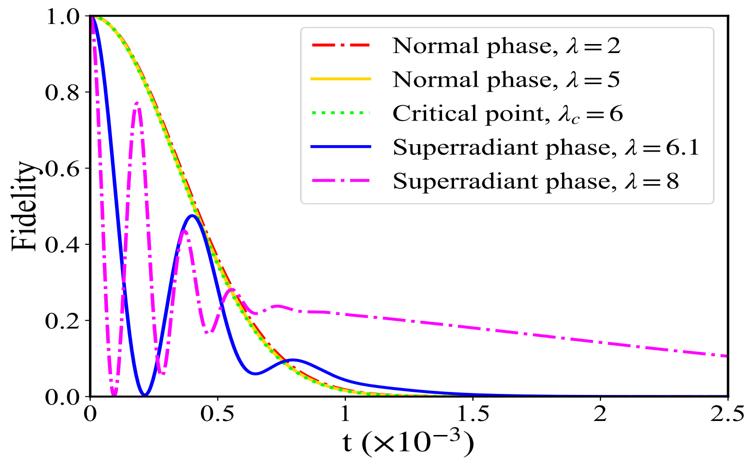

Figure 3. Variation of fidelity with time for systems with the same initial state under different phase transition parameters. The other parameters are the same as in Figures 1 and 2.

4. The Effect of Initial State Entanglement on the Evolution Speed of System Dynamics

Entanglement is a fundamental resource. In this section, we study the effect of the initial state entanglement on the evolution speed of the system dynamics in normal phase and superradiant phase systems, respectively. For the initial state represented by Equation (18), the magnitude of the initial entanglement is [97]

$$E = W^2|\sin 2\theta|\sqrt{(1-\exp(-4|\gamma|^2))(1-\exp(-4|\eta|^2)} \tag{37}$$

where W is the normalization coefficient of the initial state. When we choose $\gamma = \eta = 5$, we can obtain the relationship between the size of the initial quantum entanglement of the system and θ from Equations (19) and (37), that is $E \approx |\sin 2\theta|$. In this way, we only need to adjust the value of θ to control the size of the initial quantum entanglement.

In the following, we study the quantum speed limit time of the system in the normal phase and the superradiant phase by adjusting the initial state parameter θ. In Figure 4a, we study the variation of the system fidelity with time when the initial state entanglement takes different values. We find that, in the normal phase, the system's initial state entanglement hardly affects the system's quantum speed limit time. However, in the superradiant phase, the greater the entanglement of the initial state of the system, the shorter the time for the system to evolve to the orthogonal state of the initial state. In order to verify the above conclusion, in Figure 4b, when the initial state entanglement takes different values, we plot the fidelity of the initial state of the system as a function of time. We find that, in the normal phase, a different initial state entanglement has almost no effect on the evolution of the system dynamics. However, in the superradiant phase, larger initial state entanglement can accelerate the system dynamics' evolution. The numerical simulation of the actual dynamical evolution of the system in Figure 4b was executed with the Qutip software [96].

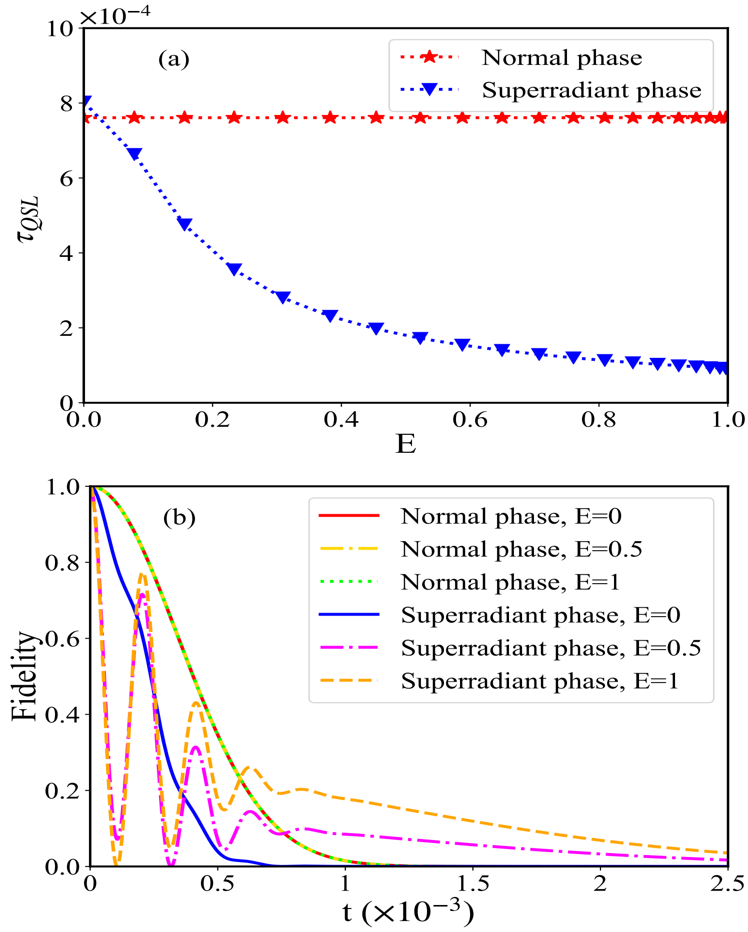

Figure 4. (**a**) Variation of the MT-type quantum velocity limit time of the system with the initial state entanglement when the system is in the normal and superradiant phases, respectively. (**b**) Fidelity of the initial state of the system with time for different initial state entanglement and different phase transition parameters. The initial state parameters of the system are $\gamma = \eta = 5$ and $\varphi = 0$. The other parameters are the same as in Figure 1.

5. Conclusions

In summary, we focused on the effect of the Dicke quantum phase transition on the quantum speed limit time of the system. We obtained the MT-type and ML-type quantum speed limit times following the general approach. We found that the MT-type quantum speed limit time is always larger than the ML-type quantum speed limit time, both in the normal and superradiant phases. Therefore, we finally chose the MT-type quantum speed limit time as the quantum speed limit time of the system. In the normal phase, the time taken for the system to evolve from the initial state to the orthogonal state of the initial state is almost independent of the phase transition parameters. However, a stronger phase transition parameter in the superradiant phase enables the system to have a shorter quantum speed limit time. In addition, we investigated the effect of the entanglement of the initial state on the quantum speed limit time. We found that, in the normal phase, the entanglement of the initial state does not affect the quantum speed limit time of the system. However, in the superradiant phase, a more extensive initial state entanglement can give the system a shorter quantum speed limit time. We verified all the above conclusions by studying the actual dynamical evolution of the system through numerical calculations.

Author Contributions: Conceptualization, W.L. and S.T.; methodology, J.Y. and Y.L.; software, C.Z., S.L. and Y.S.; validation, W.L., C.Z., Y.S., J.Y. and S.T.; formal analysis, W.L.; investigation, W.L.; resources, W.L., Y.L., Y.S., J.Y. and S.T.; data curation, C.Z. and S.L.; writing—original draft preparation, W.L. and S.T.; writing—review and editing, W.L. and C.Z.; visualization, C.Z., S.L. and Y.S.; supervision, W.L.; project administration, W.L.; funding acquisition, W.L. All authors have read and agreed to the published version of the manuscript.

Funding: This work was supported by the NSFC (Grant No. 12205092, No. 12205088, No. 11947069, and No. 11905053), the Scientific Research Fund of Hunan Provincial Education Department (Grant No. 22A0507, No. 21B0647, No. 21B0639, and No. 20C0495), and the Open fund project of the Key Laboratory of Optoelectronic Control and Detection Technology of University of Hunan Province (Grant No. 2022HSKFJJ038)

Institutional Review Board Statement: Not applicable.

Informed Consent Statement: Not applicable.

Data Availability Statement: Not applicable.

Conflicts of Interest: The authors declare no conflict of interest.

Appendix A. Specific Expression for the Average Value of $\hat{H}_{sp}^2$ over the Initial State $|\Psi(0)\rangle$

Since the average value of $\hat{H}_{sp}^2$ over the initial state $|\Psi(0)\rangle$ is too cumbersome, we give its specific expression as follows:

$$
\begin{aligned}
& \langle\Psi(0)|\hat{H}_{sp}^2|\Psi(0)\rangle \\
= \; & \cos^2\theta|A_1|^2\Big(|A_1|^2+1\Big)+\sin^2\theta|A_2|^2\Big(|A_2|^2+1\Big)+\sin 2\theta\exp\Big[-2\Big(|\alpha_1|^2+|\beta_1|^2\Big)\Big] \\
& \times\mathrm{Re}\{\exp(i\varphi)A_1^*A_2(A_1^*A_2+1)\} \\
& +\cos^2\theta|B_1|^2\Big(|B_1|^2+1\Big)+\sin^2\theta|B_2|^2\Big(|B_2|^2+1\Big)+\sin 2\theta\exp\Big[-2\Big(|\alpha_1|^2+|\beta_1|^2\Big)\Big] \\
& \times\mathrm{Re}\{\exp(i\varphi)B_1^*B_2(B_1^*B_2+1)\} \\
& +\cos^2\theta\Big(2\mathrm{Re}\Big(A_1^2\Big)+2|A_1|^2+1\Big)\Big(2\mathrm{Re}\Big(B_1^2\Big)+2|B_1|^2+1\Big) \\
& +\sin^2\theta\Big(2\mathrm{Re}\Big(A_2^2\Big)+2|A_2|^2+1\Big)\Big(2\mathrm{Re}\Big(B_2^2\Big)+2|B_2|^2+1\Big) \\
& +\sin 2\theta\exp\Big[-2\Big(|\alpha_1|^2+|\beta_1|^2\Big)\Big] \\
& \times\mathrm{Re}\Big\{\exp(i\varphi)\Big(A_1^{*2}+A_2^2+2A_1^*A_2+1\Big)\Big(B_1^{*2}+B_2^2+2B_1^*B_2+1\Big)\Big\} \\
& +\cos^2\theta\Big(6|B_1|^4+2\Big(4|B_1|^2+6\Big)\mathrm{Re}\Big(B_1^2\Big)+2\mathrm{Re}\Big(B_1^4\Big)+12|B_1|^2+3\Big) \\
& +\sin^2\theta\Big(6|B_2|^4+2\Big(4|B_2|^2+6\Big)\mathrm{Re}\Big(B_2^2\Big)+2\mathrm{Re}\Big(B_2^4\Big)+12|B_2|^2+3\Big) \\
& +\sin 2\theta\exp\Big[-2\Big(|\alpha_1|^2+|\beta_1|^2\Big)\Big] \\
& \times\mathrm{Re}\Big\{\exp(i\varphi)\Big(B_1^{*4}+4B_1^{*3}B_2+6B_1^{*2}B_2^2+4B_1^*B_2^3+B_2^4+12B_1^*B_2+6B_1^{*2}+6B_2^2+3\Big)\Big\} \\
& +\cos^2\theta|A_1|^2|B_1|^2+\sin^2\theta|A_2|^2|B_2|^2 \\
& +\sin 2\theta\exp\Big[-2\Big(|\alpha_1|^2+|\beta_1|^2\Big)\Big]\mathrm{Re}\{\exp(i\varphi)A_1^*A_2B_1^*B_2\} \\
& +4\cos^2\theta\mathrm{Re}(A_1)\mathrm{Re}(B_1)\Big(2|A_1|^2+1\Big)+4\sin^2\theta\mathrm{Re}(A_2)\mathrm{Re}(B_2)\Big(2|A_2|^2+1\Big) \\
& +\sin 2\theta\exp\Big[-2\Big(|\alpha_1|^2+|\beta_1|^2\Big)\Big]
\end{aligned}
$$

$$
\begin{aligned}
&\times\mathrm{Re}\{\exp(i\varphi)(2A_1^*A_2+1)(A_1^*+A_2)(B_1^*+B_2)\}\\
&+\cos^2\theta|A_1|^2\left(2\mathrm{Re}\left(B_1^2\right)+2|B_1|^2+1\right)+\sin^2\theta|A_2|^2\left(2\mathrm{Re}\left(B_2^2\right)+2|B_2|^2+1\right)\\
&+\sin 2\theta\exp\left[-2\left(|\alpha_1|^2+|\beta_1|^2\right)\right]\mathrm{Re}\left\{\exp(i\varphi)A_1^*A_2\left(B_1^{*2}+B_2^2+2B_1^*B_2+1\right)\right\}\\
&+4\cos^2\theta\mathrm{Re}(A_1)\mathrm{Re}(B_1)\left(2|B_1|^2+1\right)+4\sin^2\theta\mathrm{Re}(A_2)\mathrm{Re}(B_2)\left(2|B_2|^2+1\right)\\
&+\sin 2\theta\exp\left[-2\left(|\alpha_1|^2+|\beta_1|^2\right)\right]\mathrm{Re}\{\exp(i\varphi)(A_1^*+A_2)(B_1^*+B_2)(2B_1^*B_2+1)\}\\
&+\cos^2\theta\left(4\mathrm{Re}\left(B_1^2\right)\left(|B_1|^2+1\right)+4|B_1|^2\left(|B_1|^2+3/2\right)\right)\\
&+\sin^2\theta\left(4\mathrm{Re}\left(B_2^2\right)\left(|B_2|^2+1\right)+4|B_2|^2\left(|B_2|^2+3/2\right)\right)\\
&+\sin 2\theta\exp\left[-2\left(|\alpha_1|^2+|\beta_1|^2\right)\right]\\
&\times\mathrm{Re}\left\{\exp(i\varphi)\left[2(B_1^*B_2+1)\left(B_1^{*2}+B_2^2\right)+4B_1^*(B_1^*B_2+3/2)B_2\right]\right\}\\
&+4\mathrm{Re}(A_1)\left(3|B_1|^2\mathrm{Re}(B_1)+3\mathrm{Re}(B_1)+\mathrm{Re}\left(B_1^3\right)\right)\cos^2\theta\\
&+4\mathrm{Re}(A_2)\left(3|B_2|^2\mathrm{Re}(B_2)+3\mathrm{Re}(B_2)+\mathrm{Re}\left(B_2^3\right)\right)\sin^2\theta\\
&+\sin 2\theta\exp\left[-2\left(|\alpha_1|^2+|\beta_1|^2\right)\right]\\
&\times\mathrm{Re}\left\{\exp(i\varphi)(A_1^*+A_2)\left(B_1^{*3}+B_2^3+3(B_2+B_1^*)(B_1^*B_2+1)\right)\right\}.
\end{aligned}
\tag{A1}
$$

References

1. Deffner, S.; Campbell, S. Quantum speed limits: From Heisenberg's uncertainty principle to optimal quantum control. *J. Phys. A Math. Theor.* **2017**, *50*, 453001. [CrossRef]
2. Taddei, M.M.; Escher, B.M.; Davidovich, L.; de Matos Filho, R.L. Quantum Speed Limit for Physical Processes. *Phys. Rev. Lett.* **2013**, *110*, 050402. [CrossRef] [PubMed]
3. del Campo, A.; Egusquiza, I.L.; Plenio, M.B.; Huelga, S.F. Quantum Speed Limits in Open System Dynamics. *Phys. Rev. Lett.* **2013**, *110*, 050403. [CrossRef] [PubMed]
4. Caneva, T.; Murphy, M.; Calarco, T.; Fazio, R.; Montangero, S.; Giovannetti, V.; Santoro, G.E. Optimal Control at the Quantum Speed Limit. *Phys. Rev. Lett.* **2009**, *103*, 240501. [CrossRef] [PubMed]
5. Okuyama, M.; Ohzeki, M. Quantum Speed Limit is Not Quantum. *Phys. Rev. Lett.* **2018**, *120*, 070402. [CrossRef] [PubMed]
6. Jones, P.J.; Kok, P. Geometric derivation of the quantum speed limit. *Phys. Rev. A* **2010**, *82*, 022107. [CrossRef]
7. Marvian, I.; Spekkens, R.W.; Zanardi, P. Quantum speed limits, coherence, and asymmetry. *Phys. Rev. A* **2016**, *93*, 052331. [CrossRef]
8. Shanahan, B.; Chenu, A.; Margolus, N.; del Campo, A. Quantum Speed Limits across the Quantum-to-Classical Transition. *Phys. Rev. Lett.* **2018**, *120*, 070401. [CrossRef]
9. Campaioli, F.; Pollock, F.A.; Binder, F.C.; Modi, K. Tightening Quantum Speed Limits for Almost All States. *Phys. Rev. Lett.* **2018**, *120*, 060409. [CrossRef]
10. Bekenstein, J.D. Energy Cost of Information Transfer. *Phys. Rev. Lett.* **1981**, *46*, 623–626. [CrossRef]
11. Lloyd, S. Ultimate physical limits to computation. *Nature* **2000**, *406*, 1047–1054. [CrossRef]
12. Yung, M.H. Quantum speed limit for perfect state transfer in one dimension. *Phys. Rev. A* **2006**, *74*, 030303. [CrossRef]
13. Zhou, M.G.; Cao, X.Y.; Lu, Y.S.; Wang, Y.; Bao, Y.; Jia, Z.Y.; Fu, Y.; Yin, H.L.; Chen, Z.B. Experimental quantum advantage with quantum coupon collector. *Research* **2022**, *2022*, 9798679. [CrossRef] [PubMed]
14. Liu, W.B.; Li, C.L.; Xie, Y.M.; Weng, C.X.; Gu, J.; Cao, X.Y.; Lu, Y.S.; Li, B.H.; Yin, H.L.; Chen, Z.B. Homodyne Detection Quadrature Phase Shift Keying Continuous-Variable Quantum key Distribution with High Excess Noise Tolerance. *PRX Quantum* **2021**, *2*, 040334. [CrossRef]
15. Xie, Y.M.; Lu, Y.S.; Weng, C.X.; Cao, X.Y.; Jia, Z.Y.; Bao, Y.; Wang, Y.; Fu, Y.; Yin, H.L.; Chen, Z.B. Breaking the Rate-Loss Bound of Quantum Key Distribution with Asynchronous Two-Photon Interference. *PRX Quantum* **2022**, *3*, 020315. [CrossRef]
16. Levitin, L.B. Physical limitations of rate, depth, and minimum energy in information processing. *Int. J. Theor. Phys.* **1982**, *21*, 299–309. [CrossRef]
17. Lloyd, S. Computational Capacity of the Universe. *Phys. Rev. Lett.* **2002**, *88*, 237901. [CrossRef]
18. Giovannetti, V.; Lloyd, S.; Maccone, L. Quantum limits to dynamical evolution. *Phys. Rev. A* **2003**, *67*, 052109. [CrossRef]
19. Jordan, S.P. Fast quantum computation at arbitrarily low energy. *Phys. Rev. A* **2017**, *95*, 032305. [CrossRef]

20. Giovannetti, V.; Lloyd, S.; Maccone, L. Advances in quantum metrology. *Nat. Photonics* **2011**, *5*, 222–229. [CrossRef]
21. Chin, A.W.; Huelga, S.F.; Plenio, M.B. Quantum Metrology in Non-Markovian Environments. *Phys. Rev. Lett.* **2012**, *109*, 233601. [CrossRef] [PubMed]
22. Alipour, S.; Mehboudi, M.; Rezakhani, A.T. Quantum Metrology in Open Systems: Dissipative Cramér-Rao Bound. *Phys. Rev. Lett.* **2014**, *112*, 120405. [CrossRef] [PubMed]
23. Tsang, M. Quantum metrology with open dynamical systems. *New J. Phys.* **2013**, *15*, 073005. [CrossRef]
24. Deffner, S.; Lutz, E. Generalized Clausius Inequality for Nonequilibrium Quantum Processes. *Phys. Rev. Lett.* **2010**, *105*, 170402. [CrossRef]
25. Deffner, S.; Lutz, E. Thermodynamic length for far-from-equilibrium quantum systems. *Phys. Rev. E* **2013**, *87*, 022143. [CrossRef]
26. Cai, X.; Zheng, Y. Quantum dynamical speedup in a nonequilibrium environment. *Phys. Rev. A* **2017**, *95*, 052104. [CrossRef]
27. Caneva, T.; Calarco, T.; Fazio, R.; Santoro, G.E.; Montangero, S. Speeding up critical system dynamics through optimized evolution. *Phys. Rev. A* **2011**, *84*, 012312. [CrossRef]
28. Hegerfeldt, G.C. Driving at the Quantum Speed Limit: Optimal Control of a Two-Level System. *Phys. Rev. Lett.* **2013**, *111*, 260501. [CrossRef]
29. Hegerfeldt, G.C. High-speed driving of a two-level system. *Phys. Rev. A* **2014**, *90*, 032110. [CrossRef]
30. Lloyd, S.; Montangero, S. Information Theoretical Analysis of Quantum Optimal Control. *Phys. Rev. Lett.* **2014**, *113*, 010502. [CrossRef]
31. Gajdacz, M.; Das, K.K.; Arlt, J.; Sherson, J.F.; Opatrný, T.c.v. Time-limited optimal dynamics beyond the quantum speed limit. *Phys. Rev. A* **2015**, *92*, 062106. [CrossRef]
32. Mukherjee, V.; Carlini, A.; Mari, A.; Caneva, T.; Montangero, S.; Calarco, T.; Fazio, R.; Giovannetti, V. Speeding up and slowing down the relaxation of a qubit by optimal control. *Phys. Rev. A* **2013**, *88*, 062326. [CrossRef]
33. Deffner, S.; Lutz, E. Quantum Speed Limit for Non-Markovian Dynamics. *Phys. Rev. Lett.* **2013**, *111*, 010402. [CrossRef] [PubMed]
34. Cimmarusti, A.D.; Yan, Z.; Patterson, B.D.; Corcos, L.P.; Orozco, L.A.; Deffner, S. Environment-Assisted Speed-up of the Field Evolution in Cavity Quantum Electrodynamics. *Phys. Rev. Lett.* **2015**, *114*, 233602. [CrossRef] [PubMed]
35. Xu, Z.Y.; Luo, S.; Yang, W.L.; Liu, C.; Zhu, S. Quantum speedup in a memory environment. *Phys. Rev. A* **2014**, *89*, 012307. [CrossRef]
36. Zhang, Y.J.; Han, W.; Xia, Y.J.; Cao, J.P.; Fan, H. Quantum speed limit for arbitrary initial states. *Sci. Rep.* **2014**, *4*, 4890. [CrossRef]
37. Zhang, Y.J.; Han, W.; Xia, Y.J.; Cao, J.P.; Fan, H. Classical-driving-assisted quantum speed-up. *Phys. Rev. A* **2015**, *91*, 032112. [CrossRef]
38. Liu, C.; Xu, Z.Y.; Zhu, S. Quantum-speed-limit time for multiqubit open systems. *Phys. Rev. A* **2015**, *91*, 022102. [CrossRef]
39. Sun, Z.; Liu, J.; Ma, J.; Wang, X. Quantum speed limits in open systems: Non-Markovian dynamics without rotating-wave approximation. *Sci. Rep.* **2015**, *5*, 8444. [CrossRef]
40. Song, Y.J.; Kuang, L.M.; Tan, Q.S. Quantum speedup of uncoupled multiqubit open system via dynamical decoupling pulses. *Quantum Inf. Process.* **2016**, *15*, 2325–2342. [CrossRef]
41. Liu, H.B.; Yang, W.L.; An, J.H.; Xu, Z.Y. Mechanism for quantum speedup in open quantum systems. *Phys. Rev. A* **2016**, *93*, 020105. [CrossRef]
42. Wu, S.x.; Zhang, Y.; Yu, C.s.; Song, H.s. The initial state dependence of the quantum speed limit. *J. Phys. A Math. Theor.* **2014**, *48*, 045301. [CrossRef]
43. Mandelstam, L.; Tamm, I. The uncertainty relation between energy and time in non-relativistic quantum mechanics. In *Selected Papers*; Springer: Berlin/Heidelberg, Germany, 1991; pp. 115–123. [CrossRef]
44. Margolus, N.; Levitin, L.B. The maximum speed of dynamical evolution. *Phys. D Nonlinear Phenom.* **1998**, *120*, 188–195. [CrossRef]
45. Mirkin, N.; Toscano, F.; Wisniacki, D.A. Quantum-speed-limit bounds in an open quantum evolution. *Phys. Rev. A* **2016**, *94*, 052125. [CrossRef]
46. Funo, K.; Shiraishi, N.; Saito, K. Speed limit for open quantum systems. *New J. Phys.* **2019**, *21*, 013006. [CrossRef]
47. O'Connor, E.; Guarnieri, G.; Campbell, S. Action quantum speed limits. *Phys. Rev. A* **2021**, *103*, 022210. [CrossRef]
48. Pires, D.P.; Cianciaruso, M.; Céleri, L.C.; Adesso, G.; Soares-Pinto, D.O. Generalized Geometric Quantum Speed Limits. *Phys. Rev. X* **2016**, *6*, 021031. [CrossRef]
49. Nie, S.S.; Ren, F.H.; He, R.H.; Wu, J.; Wang, Z.M. Control cost and quantum speed limit time in controlled almost-exact state transmission in open systems. *Phys. Rev. A* **2021**, *104*, 052424. [CrossRef]
50. Wu, S.x.; Yu, C.s. Quantum speed limit for a mixed initial state. *Phys. Rev. A* **2018**, *98*, 042132. [CrossRef]
51. Marvian, I.; Lidar, D.A. Quantum Speed Limits for Leakage and Decoherence. *Phys. Rev. Lett.* **2015**, *115*, 210402. [CrossRef]
52. Deffner, S. Quantum speed limits and the maximal rate of information production. *Phys. Rev. Res.* **2020**, *2*, 013161. [CrossRef]
53. Campaioli, F.; Pollock, F.A.; Modi, K. Tight, robust, and feasible quantum speed limits for open dynamics. *Quantum* **2019**, *3*, 168. [CrossRef]
54. Ektesabi, A.; Behzadi, N.; Faizi, E. Improved bound for quantum-speed-limit time in open quantum systems by introducing an alternative fidelity. *Phys. Rev. A* **2017**, *95*, 022115. [CrossRef]
55. Il'in, N.; Lychkovskiy, O. Quantum speed limit for thermal states. *Phys. Rev. A* **2021**, *103*, 062204. [CrossRef]
56. García-Pintos, L.P.; Del Campo, A. Quantum speed limits under continuous quantum measurements. *New J. Phys.* **2019**, *21*, 033012. [CrossRef]

57. Sun, S.; Peng, Y.; Hu, X.; Zheng, Y. Quantum Speed Limit Quantified by the Changing Rate of Phase. *Phys. Rev. Lett.* **2021**, *127*, 100404. [CrossRef]
58. Kobayashi, K.; Yamamoto, N. Quantum speed limit for robust state characterization and engineering. *Phys. Rev. A* **2020**, *102*, 042606. [CrossRef]
59. Volya, A.; Zelevinsky, V. Invariant correlational entropy as a signature of quantum phase transitions in nuclei. *Phys. Lett. B* **2003**, *574*, 27–34. [CrossRef]
60. Emary, C.; Brandes, T. Chaos and the quantum phase transition in the Dicke model. *Phys. Rev. E* **2003**, *67*, 066203. [CrossRef]
61. Wang, T.L.; Wu, L.N.; Yang, W.; Jin, G.R.; Lambert, N.; Nori, F. Quantum Fisher information as a signature of the superradiant quantum phase transition. *New J. Phys.* **2014**, *16*, 063039. [CrossRef]
62. Yang, L.P.; Jacob, Z. Quantum critical detector: Amplifying weak signals using discontinuous quantum phase transitions. *Opt. Express* **2019**, *27*, 10482–10494. [CrossRef] [PubMed]
63. Paunković, N.; Sacramento, P.D.; Nogueira, P.; Vieira, V.R.; Dugaev, V.K. Fidelity between partial states as a signature of quantum phase transitions. *Phys. Rev. A* **2008**, *77*, 052302. [CrossRef]
64. Relaño, A.; Arias, J.M.; Dukelsky, J.; García-Ramos, J.E.; Pérez-Fernández, P. Decoherence as a signature of an excited-state quantum phase transition. *Phys. Rev. A* **2008**, *78*, 060102. [CrossRef]
65. Chen, J.J.; Cui, J.; Zhang, Y.R.; Fan, H. Coherence susceptibility as a probe of quantum phase transitions. *Phys. Rev. A* **2016**, *94*, 022112. [CrossRef]
66. Yuan, J.B.; Lu, W.J.; Song, Y.J.; Kuang, L.M. Single-impurity-induced Dicke quantum phase transition in a cavity-Bose-Einstein condensate. *Sci. Rep.* **2017**, *7*, 7404. [CrossRef]
67. Lu, W.J.; Li, Z.; Kuang, L.M. Nonlinear Dicke quantum phase transition and its quantum witness in a cavity-Bose–Einstein-condensate system. *Chin. Phys. Lett.* **2018**, *35*, 116401. [CrossRef]
68. Hu, M.L.; Gao, Y.Y.; Fan, H. Steered quantum coherence as a signature of quantum phase transitions in spin chains. *Phys. Rev. A* **2020**, *101*, 032305. [CrossRef]
69. Zhou, B.; Yang, C.; Chen, S. Signature of a nonequilibrium quantum phase transition in the long-time average of the Loschmidt echo. *Phys. Rev. B* **2019**, *100*, 184313. [CrossRef]
70. Wang, Q.; Pérez-Bernal, F. Signatures of excited-state quantum phase transitions in quantum many-body systems: Phase space analysis. *Phys. Rev. E* **2021**, *104*, 034119. [CrossRef]
71. Quan, H.T.; Song, Z.; Liu, X.F.; Zanardi, P.; Sun, C.P. Decay of Loschmidt Echo Enhanced by Quantum Criticality. *Phys. Rev. Lett.* **2006**, *96*, 140604. [CrossRef]
72. Wu, W.; Xu, J.B. Geometric phase, quantum Fisher information, geometric quantum correlation and quantum phase transition in the cavity-Bose–Einstein-condensate system. *Quantum Inf. Process.* **2016**, *15*, 3695–3709. [CrossRef]
73. Wang, Q.; Pérez-Bernal, F. Excited-state quantum phase transition and the quantum-speed-limit time. *Phys. Rev. A* **2019**, *100*, 022118. [CrossRef]
74. Heyl, M. Quenching a quantum critical state by the order parameter: Dynamical quantum phase transitions and quantum speed limits. *Phys. Rev. B* **2017**, *95*, 060504. [CrossRef]
75. Wei, Y.B.; Zou, J.; Wang, Z.M.; Shao, B. Quantum speed limit and a signal of quantum criticality. *Sci. Rep.* **2016**, *6*, 19308. [CrossRef] [PubMed]
76. Rodriguez, J.P.J.; Chilingaryan, S.A.; Rodríguez-Lara, B.M. Critical phenomena in an extended Dicke model. *Phys. Rev. A* **2018**, *98*, 043805. [CrossRef]
77. Guerra, C.A.E.; Mahecha-Gómez, J.; Hirsch, J.G. Quantum phase transition and Berry phase in an extended Dicke model. *Eur. Phys. J. D* **2020**, *74*, 1–7. [CrossRef]
78. Stitely, K.C.; Giraldo, A.; Krauskopf, B.; Parkins, S. Nonlinear semiclassical dynamics of the unbalanced, open Dicke model. *Phys. Rev. Res.* **2020**, *2*, 033131. [CrossRef]
79. Shao, Y.; Liu, B.; Zhang, M.; Yuan, H.; Liu, J. Operational definition of a quantum speed limit. *Phys. Rev. Res.* **2020**, *2*, 023299. [CrossRef]
80. Shao, L.; Zhang, R.; Lu, W.; Zhang, Z.; Wang, X. Quantum phase transition in XXZ central spin model. *arXiv* **2022**, arXiv:2207.04191.
81. Wang, Q. Quantum Chaos in the Extended Dicke Model. *Entropy* **2022**, *24*, 1415. [CrossRef]
82. Lu, W.; Zhai, C.; Liu, Y.; Song, Y.; Yuan, J.; Tang, S. Berry Phase of Two Impurity Qubits as a Signature of Dicke Quantum Phase Transition. *Photonics* **2022**, *9*, 844. [CrossRef]
83. Braunstein, S.L.; Kimble, H.J. Teleportation of Continuous Quantum Variables. *Phys. Rev. Lett.* **1998**, *80*, 869–872. [CrossRef]
84. Cerf, N.J.; Ipe, A.; Rottenberg, X. Cloning of Continuous Quantum Variables. *Phys. Rev. Lett.* **2000**, *85*, 1754–1757. [CrossRef] [PubMed]
85. Brennecke, F.; Ritter, S.; Donner, T.; Esslinger, T. Cavity Optomechanics with a Bose-Einstein Condensate. *Science* **2008**, *322*, 235–238. [CrossRef] [PubMed]
86. De Chiara, G.; Paternostro, M.; Palma, G.M. Entanglement detection in hybrid optomechanical systems. *Phys. Rev. A* **2011**, *83*, 052324. [CrossRef]
87. Asjad, M.; Saif, F. Engineering entanglement mechanically. *Phys. Lett. A* **2012**, *376*, 2608–2612 [CrossRef]

88. Asjad, M.; Shahzad, M.A.; Saif, F. Quantum degenerate Fermi gas entanglement in optomechanics. *Eur. Phys. J. D* **2013**, *67*, 1–5. [CrossRef]
89. Asjad, M.; Saif, F. Steady-state entanglement of a Bose-Einstein condensate and a nanomechanical resonator. *Phys. Rev. A* **2011**, *84*, 033606. [CrossRef]
90. Asjad, M.; Qasymeh, M.; Eleuch, H. Continuous-Variable Quantum Teleportation Using a Microwave-Enabled Plasmonic Graphene Waveguide. *Phys. Rev. Appl.* **2021**, *16*, 034046. [CrossRef]
91. Musadiq, M.; Khan, S. Quantum speed limit time, non-Markovianity, and quantum phase transition of the Dicke model. *JOSA B* **2020**, *37*, 2930–2935. [CrossRef]
92. Fröhlich, H. Theory of the Superconducting State. I. The Ground State at the Absolute Zero of Temperature. *Phys. Rev.* **1950**, *79*, 845–856. [CrossRef]
93. Nakajima, S. Perturbation theory in statistical mechanics. *Adv. Phys.* **1955**, *4*, 363–380. [CrossRef]
94. Holstein, T.; Primakoff, H. Field Dependence of the Intrinsic Domain Magnetization of a Ferromagnet. *Phys. Rev.* **1940**, *58*, 1098–1113. [CrossRef]
95. Baumann, K.; Guerlin, C.; Brennecke, F.; Esslinger, T. Dicke quantum phase transition with a superfluid gas in an optical cavity. *Nature* **2010**, *464*, 1301–1306. [CrossRef]
96. Johansson, J.R.; Nation, P.D.; Nori, F. QuTiP: An open-source Python framework for the dynamics of open quantum systems. *Comput. Phys. Commun.* **2012**, *183*, 1760–1772. [CrossRef]
97. Kuang, L.M.; Zhou, L. Generation of atom–photon entangled states in atomic Bose-Einstein condensate via electromagnetically induced transparency. *Phys. Rev. A* **2003**, *68*, 043606. [CrossRef]